24th COBEM - 2017

24th ABCM International Congress of Mechanical Engineering
December 3-8, 2017, Curitiba, PR, Brazil

COBEM-2017-0480
NUMERICAL SIMULATION OF WIND FLOW OVER A HIGHLY COMPLEX TOPOGRAPHY: THE BOLUND HILL CASE

William Correa Radunz
Adriane Prisco Petry
Federal University of Rio Grande do Sul, Department of Mechanical Engineering (DEMEC), R. Sarmento Leite, 425, 90050-170, Rio Grande do Sul, Brazil
william.radunz@ufrgs.br
adrianep@mecanica.ufrgs.br

Abstract. *The feasibility or modern wind power plants is directly related to the accuracy with which the wind resource is quantified at the proposed site. Numerical wind flow modeling with Computational Fluid Dynamics (CFD) has become the rule for resource assessment in complex sites, and high-quality atmospheric-scale experiments enable the development of increasingly accurate models. The Bolund hill experiment consists of one of the most valuable sources of data in complex terrain. In this paper, the the Atmospheric Surface Layer wind flow over Bolund hill was simulated with a consistent combination of turbulence model, wall-functions and inflow conditions by using the C++ toolbox OpenFOAM. A number of grids and $k-\epsilon$ model constants were used so as to evaluate the sensitivity to the inputs and determine the most sensible choice of parameters. The modified models displayed better agreement with the data, although they substantially failed to predict the TKE levels immediately after the leading edge of the hill and further model development is necessary.*

Keywords: *wind flow, OpenFOAM, Bolund hill*

1. INTRODUCTION

There is a growing demand in the wind energy community for the development of more accurate wind flow models in order to plan improved wind power plant layouts and reduce the uncertainty in the wind resource. Historically, these wind flow models gained notice in the mid 70s through the work of Jackson and Hunt (1975). The models employed consisted mostly of linearized versions of the Navier-Stokes equations, and were devised for attached flows with small terrain perturbations. When faced with terrains of higher complexity, the linear models tended to overpredict the wind speeds at the top of elevations which led to the development of different models which were based on Computational Fluid Dynamics (CFD). The work of Raithby *et al.* (1987) is possibly the first high-impact application of CFD on micro-scale wind flow simulation, and since then the field expanded considerably.

Although CFD is theoretically capable of predicting non-linear phenomena, most of the turbulence models were developed and validated for applications on a scale much smaller than the atmospheric scale and, thus, require further development and assessment. Atmospheric-scale experiments consist of a valuable, although intensive and expensive, source of data for model evaluation and development. In 2011, a major experiment entitled the Bolund hill project aimed at measuring and analyzing the wind micro climate near a sharp hill near a coast in Denmark, which is detailed in the work of Berg *et al.* (2011) and Bechmann *et al.* (2011). Bolund and its surroundings are a reliable resource for model evaluation since the hill surface is well detailed and the incoming wind is mostly undisturbed and fully-developed.

In the present study, the open-source C++ toolbox OpenFOAM is used as the environment for wind flow model development. The library has a number of peculiarities which are inviting for model development, which include the freely-editable state-of-the-art CFD and field operations code. The work presented here includes the modifications of some of the code wall-functions, the methodology for selecting the $k-\epsilon$ turbulence model constants and the evaluation of model sensitivity to the grid and the aforementioned constants. In section 2. the governing equations of the CFD model are presented alongside the inflow profiles and wall-functions. The domain and boundary conditions based on the measurements are discussed in section 3. Results are compared to the measured data and discussed in 4. Conclusions and highlights of this work are found in section 5.

2. GOVERNING EQUATIONS

According to Stull (2017), the ASL is the lowest portion of the ABL and where the surface effects like friction and heat convection have a major effect on the wind speed and other fields, which change substantially with height. One

peculiarity of the ASL is that turbulent *momentum* and heat fluxes are somewhat uniform with height, which is why it is also known as constant flux layer. By neglecting the Coriolis force and stratification effects, the lowest 200 m of the ABL can be modeled by the standard $k-\epsilon$ turbulence model which is shown in index notation below

$$\nu_t = C_\mu \frac{k^2}{\epsilon} \tag{1}$$

$$\frac{\partial}{\partial x_i}(U_i k) = \frac{\partial}{\partial x_j}\left[\left(\nu + \frac{\nu_t}{\sigma_k}\right)\frac{\partial k}{\partial x_j}\right] + G_k - \epsilon \tag{2}$$

$$\frac{\partial}{\partial x_i}(U_i \epsilon) = \frac{\partial}{\partial x_j}\left[\left(\nu + \frac{\nu_t}{\sigma_\epsilon}\right)\frac{\partial \epsilon}{\partial x_j}\right] + C_{\epsilon 1} G_k \frac{\epsilon}{k} - C_{\epsilon 2}\frac{\epsilon^2}{k} \tag{3}$$

$$G_k = \nu_t \left(\frac{\partial U_i}{\partial x_j} + \frac{\partial U_j}{\partial x_i}\right)\frac{\partial U_i}{\partial x_j} \tag{4}$$

where ν_t is the turbulence kinematic viscosity, k is the turbulence kinetic energy (TKE) and ϵ its dissipation rate, U is the Reynolds-Averaged wind speed, ν is the kinematic viscosity of the air and G_k is the TKE production term. The standard model constants based on the work of Launder and Spalding (1974) are the following:

$$C_{\epsilon 1} = 1.44, \quad C_{\epsilon 2} = 1.92, \quad C_\mu = 0.09, \quad \sigma_k = 1.0, \quad \sigma_\epsilon = 1.3 \tag{5}$$

These classic constants are usually modified for micro-scale atmospheric flow simulation since they were adjusted to engineering-scale flows. Richards and Norris (2011) elucidate that C_μ may be adjusted to fit the TKE in the atmosphere, but the turbulent Prandtl number of the dissipation rate ought to be corrected

$$C_\mu = \frac{u_\star^4}{k^2} \tag{6}$$

$$\sigma_\epsilon = \frac{\kappa^2}{(C_{\epsilon 2} - C_{\epsilon 1})\sqrt{C_\mu}} \tag{7}$$

3. DOMAIN AND BOUNDARY CONDITIONS

According to Berg *et al.* (2011), the Bolund hill consists, in fact, of a 12 m escarpment surrounded mostly by the sea. This is shown in Fig. 1. The scale of Bolund ensures that it is thoroughly immerse in the atmospheric surface layer and, thus, that the flow can be modeled as neutrally stratified. The westerly winds that come from the sea are valuable for wind flow modeling since these are mostly equilibrium, undisturbed neutrally-stratified profiles which allow for a reliable inflow condition in the numerical model. In addition, Bolund is homogeneously covered with grass and has no obstacles so that a uniform roughness $z_0 = 0.015$ m parametrization may be applied. Still according to Berg *et al.* (2011), the sea surface roughness can be set as $z_0 = 0.0003$ m. The same value is employed for the log-law at the inflow condition.

In the present study, the wind incoming from direction 270° (along line B in Fig. 2) is simulated. The inflow parameters are based on the measurements performed at the mast M0 and are plotted alongside a number of fitted profiles in Fig. 3. It should be emphasized that, although the best fit to the data was found for the profiles "Fitted" and "Bechmann", the "Bechmann suggested" was used in the simulations. This is due to the fact that in the work of Bechmann *et al.* (2011), as well as other papers on the simulation of Bolund hill, these are the conditions employed, and, thus, the present results may be straightforwardly assessed. The computational domain consists of a box centered on the hill and which has the surroundings elevation at its bottom. The Digital Elevation Model (DEM) based on Bolund which represents the base of the grid is shown in Fig. 4. Regarding the meshing strategy, the OpenFOAM application for the generation of unstrucuted grids *snappyHexMesh* was used. The sides and top of the domain are set as free-slip walls, constant pressure at the outlet and the classic Richards and Hoxey (1993) equilibrium profiles at the inlet. Under the assumptions of negligible vertical velocity, constant pressure and constant shear stress, the following set of inflow profiles are a solution to Eqs. (2) and (3)

$$u = \frac{u_\star}{\kappa} ln\left(\frac{z + z_0}{z_0}\right) \tag{8}$$

$$k = \frac{u_\star^2}{\sqrt{C_\mu}} \tag{9}$$

$$\epsilon = \frac{u_\star^3}{(z + z_0)} \tag{10}$$

Even though these profiles should remain unchanged if the terrain is plain and there is no change in surface roughness, they may change due to an inconsistency between turbulence model, inflow conditions and WFs. Authors like Parente *et al.* (2011) and Balogh *et al.* (2012) demonstrated that consistency between the $k-\epsilon$ model and wall-functions could be achieved adding z_0 to the height in the ϵ field wall-function as follows

$$\epsilon_P = \frac{C_\mu^{0.75} k^{1.5}}{\kappa(z_P)} \rightarrow \frac{C_\mu^{0.75} k^{1.5}}{\kappa(z_P + z_0)} \tag{11}$$

$$G_{k_P} = \frac{\tau_w^2}{\kappa C_\mu^{0.25} k_P^{0.5}(z_P)} \rightarrow \frac{\tau_w^2}{\kappa C_\mu^{0.25} k_P^{0.5}(z_P + z_0)} \tag{12}$$

The remaining wall-function, in this particular formulation the turbulent viscosity ν_t *nutkAtmRoughWallFunction* in OpenFOAM, is already consistent with the model and inflow conditions are required no further development. The aforementioned wall-functions were employed on the sea and Bolund surfaces. In order to evaluate the model sensitivity and realize the most sensible choice for the constants of the $k-\epsilon$ model, three set-ups were used and can be seen in Tab. 1. The first model configuration named "Standard" used the standard $k-\epsilon$ constants proposed by Launder and Spalding (1974). The second, named "Atmospheric", is based on the work of Beljaars *et al.* (1987) which suggested this constants were more appropriate to atmospheric flows and have been widely used in the wind energy and engineering community. Lastly is the "Fitted" formulation, which calculated the model constant C_μ by fitting Eq. 6 to the TKE k_{ref} suggested by Bechmann *et al.* (2011).

Figure 1. Bolund hill and surroundings. Taken from Berg *et al.* (2011).

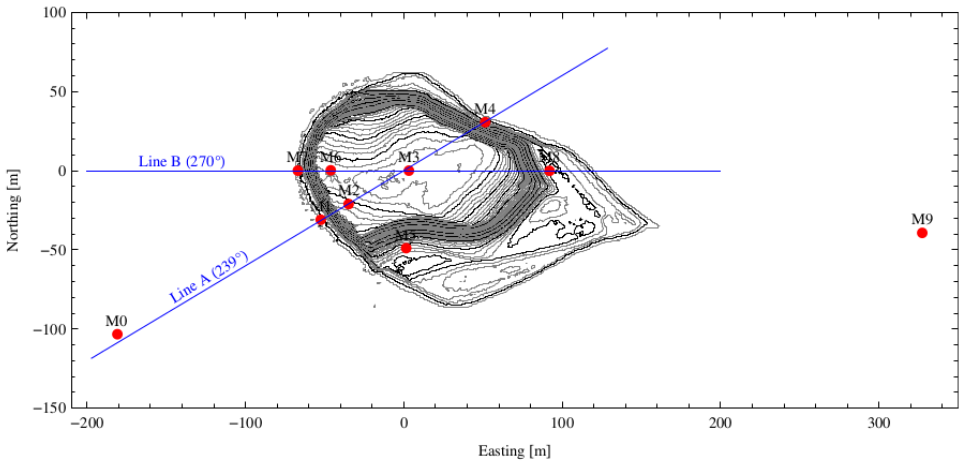

Figure 2. Bolund hill contour-lines and measuring towers. Taken from Berg *et al.* (2011).

Table 1. Inflow and model parameters used in the simulations

Model	z_0 $[m]$	u^* $[m\ s^{-1}]$	C_μ	σ_ϵ	k_{ref} $[m^2\ s^{-2}]$
Standard	0.0003	0.40	0.090	1.30	0.533
Atmospheric	0.0003	0.40	0.033	1.835	0.881
Fitted (Bechmann REF)	0.0003	0.40	0.0297	1.933	0.928

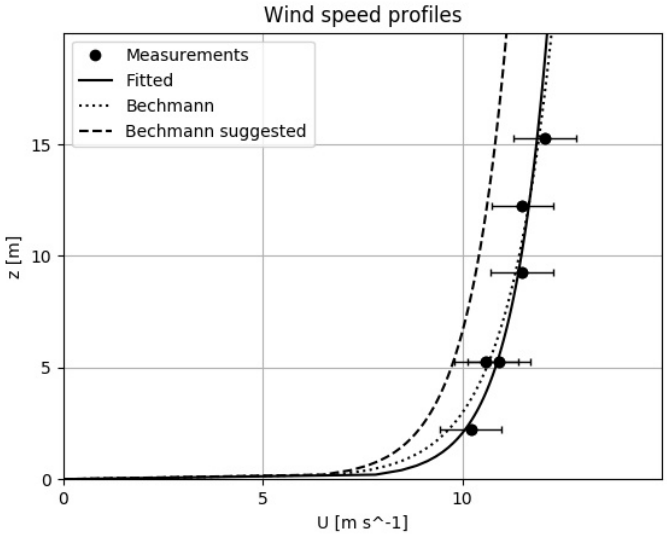

Figure 3. Wind speed data measured at mast M0. The profile "Bechmann suggested" was used for the simulations in this paper.

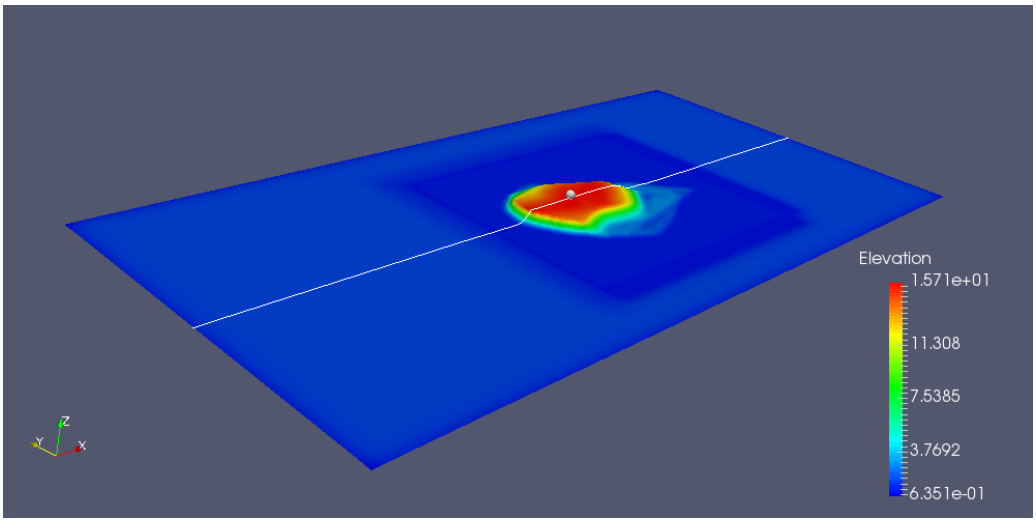

Figure 4. Bolund hill DEM.

4. RESULTS

The OpenFOAM solver *simpleFoam* was used for all the simulations in this section. It consists of a steady-state, incompressible, turbulent-flow solver which suits the modeling of the neutral ASL. The convection scheme was set as upwind for the U, k and ϵ fields. In what concerns the solvers, the Generalised Geometric-Algebraic Multi-Grid (GAMG) was used for pressure, whilst the Preconditioned Bi-Conjugate Gradient (PBiCG) was employed for the remaining fields. The solver convergence criteria was defined as 1E-4 for all fields with 0.3 relaxation factor for pressure and 0.7 for the remaining fields. The CFD simulations were carried on a desktop computer with 8 4GHz cores and 16GB RAM in parallel.

In general, the model employed displayed good agreement with the data along line B 2 m above ground level in term of relative speed-up (RSU). It can be seen in Fig. 5 that the RSU decreased smoothly as the hill front was approached due to the obstruction Bolund imposes on the flow. Upstream, therefore, the models behaved similarly an matched the measurement. Immediately after the front edge, there was a peak in the RSU and greater spread in the results. The Atmospheric and Blind (M3) set-ups closely matched the data, followed by Standard (M3) model with also good performance. As the flow proceeds to the hill center, the RSU increased monotonically and underestimated the wind speeds. Downstream of the center, the models showed akin behavior until the lee was reached and the wind speeds fell substantially. The Atmospheric and Blind configurations closely matched the data, whereas the Standard model quickly overestimated the data.

Five meters above ground, the models showed less sensitivity to grid resolution and coefficients, only differing slightly in the lee. The models underpredicted the wind speed at the M6 mast altogether and closely matched the measurements at both M7 and M3. In the lee (M8), the models Atmospheric and Blind matched the measurement but the Standard model quickly overestimated the RSU. This is shown in Fig. 6.

In Fig. 7, the relative increase in TKE 2 m above ground in displayed. The turbulence levels in the atmosphere approached the hill nearly constant and then peaked just downstream the front edge. Near the front edge, the results underestimated the TKE considerably and also shown increased sensitivity to the mesh density and turbulence model coefficients. Near the hill center the models closely matched the measurement but for the Standard model, which quickly overpredicted the relative increase in TKE. Downstream of the hill center, the Standard model performed better than the other models, which underpredicted the TKE.

Regarding the TKE levels 5 m above ground, it may be seen in Fig. 8 that the Atmospheric and Blind models closely matched the measurements at the masts M7 and M3, whilst slightly overestimated at M6. In the lee, at the mast M8, the three models underpredicted the TKE.

In order to summarize the results and obtain a better picture of the wind behavior near the hill, the RSU profiles were drawn at the masts M7, M6, M3 and M8, which is shown in Fig. 9. The profiles appeared to be consistent with the measurements but for masts M6 and M3. Whilst the model showed mostly an analogous behavior, the Atmospheric and Fitted were in better agreement with the data at mast M8. The relative increase in TKE profiles were plotted in a analogous fashion to the RSU profiles, and are displayed in Fig. 10. The TKE behavior is captured quite well at masts M7 and M3, whereas the models fail to reproduce the peak near ground at M6. In the lee of the hill, the Standard model better fitted the data near the ground and the models altogether underestimated the TKE.

The performance of the simulated cases was also evaluated using the metrics Hit Rate (HR) and relative error (e). For the HR, if the simulated results fall within one standard deviation from the data, the value 1 is assigned, otherwise, 0 is assigned. Such a procedure is carried for the wind speed and TKE fields, and calculates which percentage of the results are in reasonable agreement with the data. To quantify the deviation from the measurements, the relative error was also calculated and, together with the HR, is shown in Tab. 3. According to the results, the HR increased whilst the relative error was reduced with finer grids in for all cases. It can be observed that the cases Atmospheric and Fitted displayed a considerably better HR and e when contrasted with the Standard case. Although most statistics improved with grid refinement, the mean relative error e_U and the maximum relative error $e_{U,max}$ have risen substantially for the Atmospheric and Fitted cases.

Table 2. Numerical grids employed in the sensitivity analysis

Mesh	Volumes	ΔZ_w^* $[m]$	Domain Size [m]
M1	1,007,129	0.2	800 x 800 x 200
M2	1,495,245	0.1	800 x 800 x 200
M3	2,301,215	0.05	800 x 800 x 200

*Height of the first cell above ground.

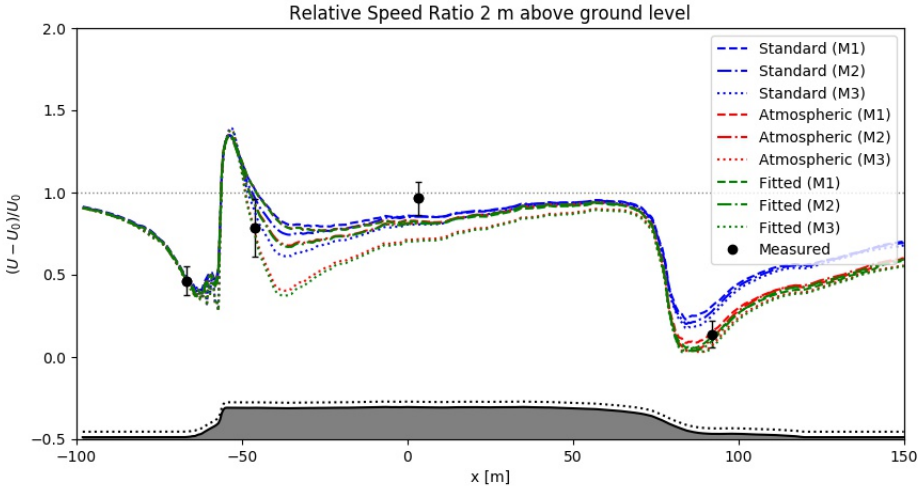

Figure 5. Relative speed-up along line B 2 m above ground level.

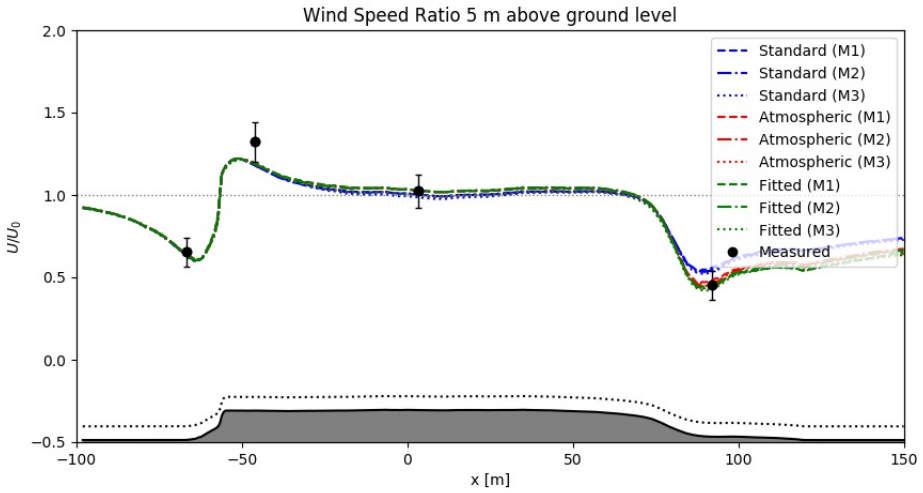

Figure 6. Relative speed-up along line B 5 m above ground level.

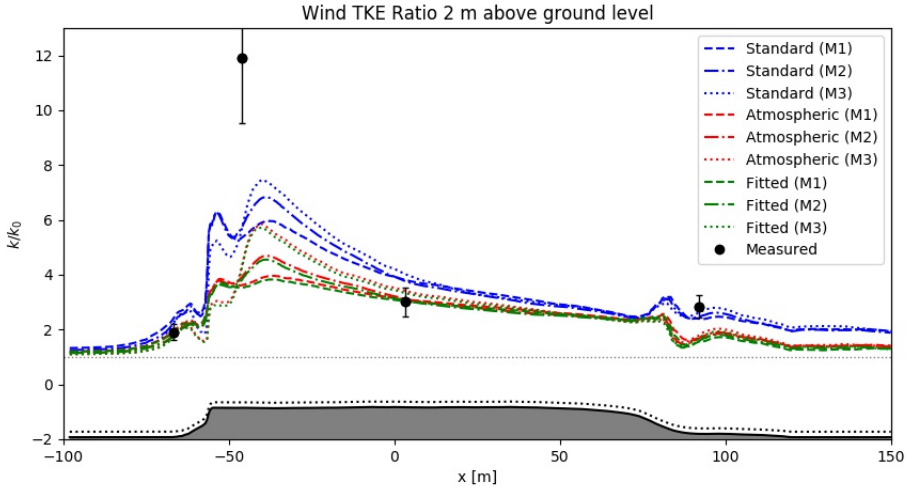

Figure 7. Relative increase in TKE along line B 2 m above ground level.

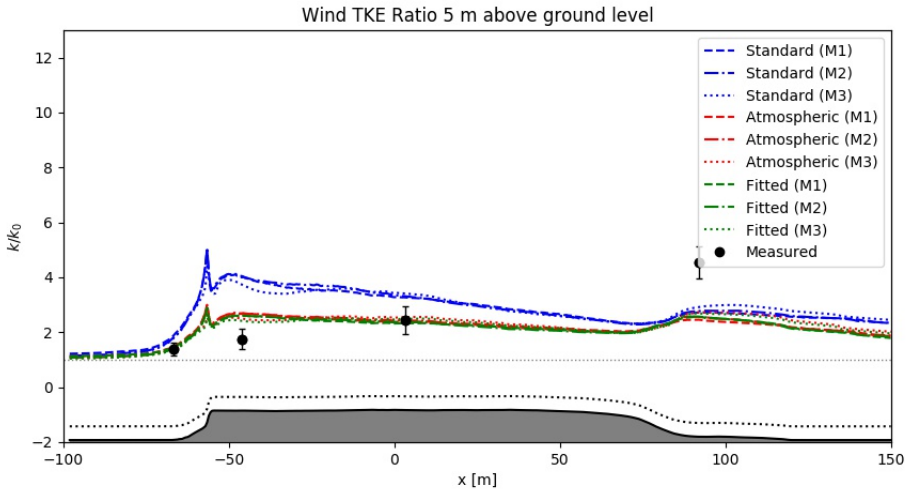

Figure 8. Relative increase in TKE along line B 5 m above ground level.

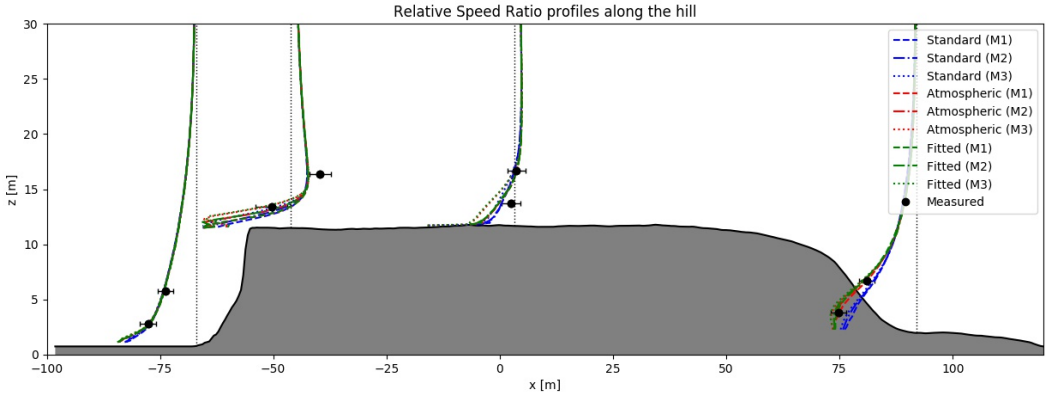

Figure 9. Relative speed-up profiles at M7, M6, M3 and M8.

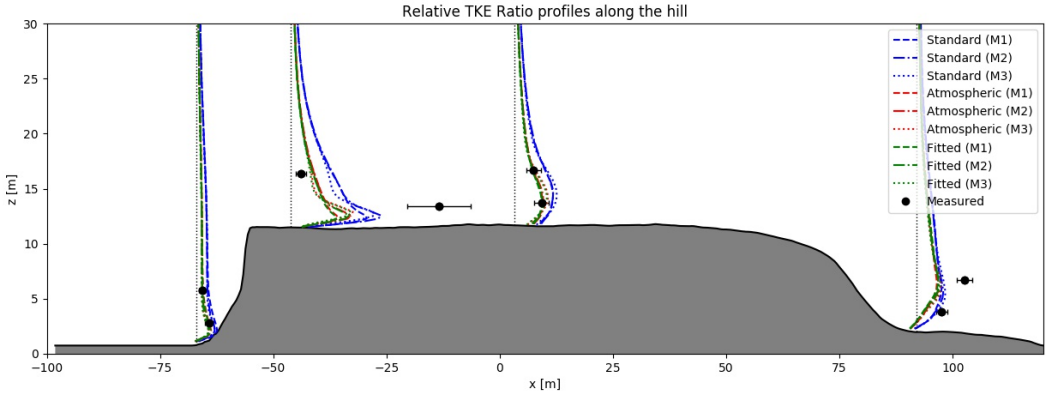

Figure 10. Relative increase in TKE profiles at M7, M6, M3 and M8.

Table 3. Hit rates and relative errors for the simulated cases

Model	HR_U [%]	e_U [%]	$e_{U,max}$ [%]	HR_k [%]	e_k [%]	$e_{k,max}$ [%]
Standard (M1)	37	26	124	0	44	128
Standard (M2)	37	21	100	12	42	130
Standard (M3)	62	18	81	25	40	113
Atmospheric (M1)	62	9	29	50	27	69
Atmospheric (M2)	75	8	18	50	27	67
Atmospheric (M3)	75	12	48	50	26	63
Fitted (M1)	62	8	29	50	27	70
Fitted (M2)	75	9	28	50	27	67
Fitted (M3)	75	14	58	50	26	64

5. CONCLUSIONS

The present work was concerned with the numerical simulation of the ASL wind flow over the orographycally-complex Bolund hill. A coherent set of $k-\epsilon$ constants, wall-functions and inflow conditions was ensured by using the atmospheric-scale wall-functions for ν_t and ϵ. The former had already been implemented in OpenFOAM, whilst the latter had to be modified. Subsequently, the sensitivity of the consistent model was evaluated by using different turbulence model constants (C_μ and σ_ϵ) and grid resolutions.

Generally, the three models employed captured reasonably well the speed-ups and increase in TKE, but significantly underpredicted the TKE measurements right after the front edge, where flow detachment is most likely to happen. In that same region, there was found great deviation amongst the results due to grid refinement and model constants. As a general trend amongst the assessed profiles, the Standard case predicted the highest TKE values at all points and displayed least proximity to the data. The Atmospheric and Fitted models showed results more akin to the data, which has ultimately led to improved hit rates and relative errors. In these cases, the HR was 75 % and 50 % whilst for the Standard model the best value found was 62 % and 25 %, for the wind speed and TKE fields, respectively. Berg *et al.* (2011) have compared

a number of linear, two-equation RANS and Large-Eddy Simulation (LES) models employed to simulate the wind flow over Bolund hill and, overall, the results found in this paper have been found to be consistent with those.

Despite the fact that the Atmospheric and Fitted cases were able to capture the wind behavior reasonably well, further model development is required to overcome the encountered weaknesses which were found immediately downstream of the lead edge and in the lee. It is still unclear whether the standard $k - \epsilon$ model, or other RANS-based models, can be improved in order to achieve the demanded accuracy. In future works, one of the major analyses to be made is concerned with the model sensitivity to discretization scheme and the influence of the grid type and resolution.

6. ACKNOWLEDGEMENTS

The authors would kindly like to thank Berg *et al.* (2011) for the data provided from the Bolund hill project, and also to the Brazilian National Council for Scientific and Technological Development (CNPq).

7. REFERENCES

Balogh, M., Parente, A. and Benocci, C., 2012. "Rans simulation of abl flow over complex terrains applying an enhanced $k - \epsilon$ model and wall function formulation: Implementation and comparison for fluent and openfoam". *Journal of Wind Engineering and Industrial Aerodynamics*, Vol. 104-106, pp. 360–368.

Bechmann, A., SÃ¿rensen, N.N., Berg, J., Mann, J. and RÃl'thorÃl', P.E., 2011. "The bolund experiment, part ii: Blind comparison of microscale flow models". *Boundary-Layer Meteorology*, Vol. 141, pp. 245–271.

Beljaars, A.C.M., Walmsley, J.L. and Taylor, P.A., 1987. "A mixed spectral finite-difference model for neutrally stratified boundary-layer flow over roughness changes and topography". *Boundary-Layer Meteorology*, Vol. 38, pp. 273–303.

Berg, J., Mann, J., Bechmann, A., Courtney, M. and JÃ¿rgensen, M., 2011. "The bolund experiment, part i: Flow over a steep, three-dimensional hill". *Boundary-Layer Meteorology*, Vol. 141, pp. 219–243.

Jackson, P.S. and Hunt, J.C.R., 1975. "Turbulent windflow over a low hill". *Quarterly Journal of the Royal Meteorology Society*, Vol. 101, pp. 929–955.

Launder, B.E. and Spalding, D.B., 1974. "The numerical computation of turbulent flows". *Computer Methods in Applied Mechanics and Engineering*, Vol. 3, pp. 269–289.

Parente, A., GorlÃl', C., van Beeck, J. and Benocci, C., 2011. "Improved $k - \epsilon$ model and wall function formulation for the rans simulation of abl flows". *Journal of Wind Engineering and Industrial Aerodynamics*, Vol. 99, pp. 267–278.

Raithby, G.D., Stubley, G.D. and Taylor, P.A., 1987. "The askervein hill project: A finite control volume prediction of three-dimensional flows over the hill". *Boundary-Layer Meteorology*, Vol. 39, pp. 247–267.

Richards, P.J. and Hoxey, R., 1993. "Appropriate boundary conditions for computational wind engineering models using the $k - \epsilon$ turbulence model". *Journal of Wind Engineering and Industrial Aerodynamics*, Vol. 47, pp. 145–153.

Richards, P.J. and Norris, S.E., 2011. "Appropriate boundary conditions for computational wind engineering models revisited". *Journal of Wind Engineering and Industrial Aerodynamics*, Vol. 99, pp. 257–266.

Stull, R., 2017. *Practical Meteorology: An Algebra-based Survey of Atmospheric Science*. University of British Columbia, 1st edition.

8. RESPONSIBILITY NOTICE

The authors are the only responsible for the printed material included in this paper.